

## Calorimetric Power Loss Measurement for Highly Efficient Converters

D. Christen, U. Badstuebner, J. Biela, and J.W. Kolar  
Power Electronic Systems Laboratory, ETH Zurich  
Physikstrasse 3, 8092 Zurich, Switzerland  
Email: chdaniel@ee.ethz.ch; www.pes.ee.ethz.ch

„This material is posted here with permission of the IEEE. Such permission of the IEEE does not in any way imply IEEE endorsement of any of ETH Zürich’s products or services. Internal or personal use of this material is permitted. However, permission to reprint/republish this material for advertising or promotional purposes or for creating new collective works for resale or redistribution must be obtained from the IEEE by writing to [pubs-permission@ieee.org](mailto:pubs-permission@ieee.org).

By choosing to view this document you agree to all provisions of the copyright laws protecting it.”

# Calorimetric Power Loss Measurement for Highly Efficient Converters

D. Christen, U. Badstuebner, J. Biela, and J.W. Kolar

Power Electronic Systems Laboratory, ETH Zurich

Physikstrasse 3, 8092 Zurich, Switzerland

Email: chdaniel@ee.ethz.ch; www.pes.ee.ethz.ch

**Abstract**—The electrical determination of power losses by measuring the input and output power can reach sufficient accuracy for DC-DC converter systems, if well calibrated voltage meters and shunt resistors are applied. However, it is difficult to determine the power in AC-systems, especially with harmonics, due to phase-errors in the electric measurement. In addition, the electromagnetic interference (EMI) of switched-mode power supplies can disturb the electric power measurement.

In this paper, the calorimetric determination of power converter system losses resulting in a high accuracy and which is almost immune against EMI phase errors, is described. The closed-type calorimeter is realized with a double-jacketed chamber which enables the power loss measurement between 10 W and 200 W for power converter systems of several kW. The resulting deviation of the implemented measurement system is less than  $\pm 0.4$  W, or  $\pm 0.05\%$  at full load conditions (several kW), respectively, over the entire measurement range.

## I. INTRODUCTION

Due to the increasing efficiency of power electronic systems, the exact determination of power losses becomes more and more important. The electrical measurement of power losses in power electronic systems by subtracting the output power from the input power is often subject to large measurement errors due to phase-errors in the measurement in AC-systems or noise caused by high frequency effects (EMI).

Calorimetric methods which allow the direct thermal measurement of losses occurring in power electronic systems are described e.g. in [?], [1], [2] as an alternative. These calorimetric methods do not depend on measured phase angles between currents and voltages and offer a very high accuracy for power measurement. Previous works describe many low power calorimeters which have an accuracy better than 0.4 W with a measurement range lower than 50 W [3]–[5]. In [6] a calorimeter is presented which is capable of measuring power losses of several mW with an accuracy of  $\pm 1.3$  mW at losses of 24 mW. Other calorimeters for high power applications e.g. induction machines and motors with power losses of 500 W and higher achieve an accuracy of better than 2% based on the measured power losses ([7]–[10]). An overview over the different calorimeters and their accuracies is given in Fig. 1.

The reference test device for the design of the presented calorimeter is a highly efficient DC-DC converter with a volume of 180 mm  $\times$  106 mm  $\times$  120 mm, an output power of 5 kW and an planned efficiency of 99.1% [11]. The planned accuracy for the calorimeter presented is better than 0.05% with respect to the full load power of the tested device. The measurement range required respectively the expected power

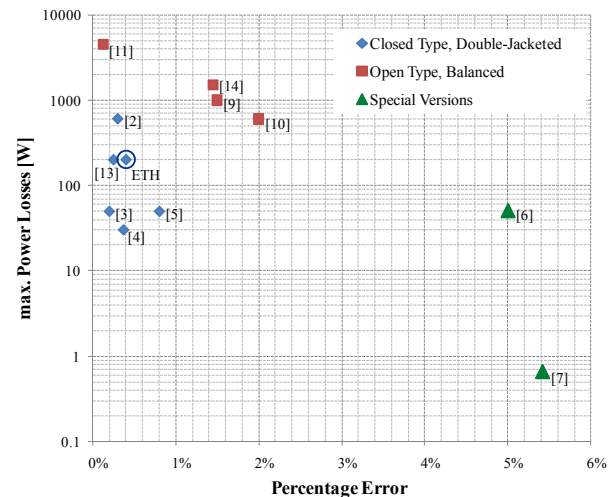


Figure 1. Overview of different implemented calorimeters and their reached accuracy. While the open type calorimeters (red) are used for high power measurements of several hundred watts, the closed type calorimeters (blue) are used for low power measurements. There are two special calorimeters (green) whereas [5] has a very short response time ( $< 2$  hours) and [6] is used for very low power measurement ( $< 650$  mW). The presented calorimeter is marked with a blue circle.

losses are between 10 W up to at least 100 W. Therefore, the following specifications can be formulated

- Accuracy better than 0.05% of the output power ( $< 2.5$  W at 5 kW)
- Measurement range between 10 W and 100 W
- Test chamber volume  $> 2.5$  dm<sup>3</sup>

Based on [2], [12] and [?], a double-jacketed calorimeter for measuring the power losses in converters (1 kW up to 10 kW output power) with an efficiency higher than 99% is described in this paper. The accuracy reached is better than  $\pm 0.4$  W at power losses from 10 W up to 100 W. By integrating a controllable pump in this water-based calorimeter higher power levels can also be measured. Furthermore, the error analysis and the implementation of the calorimeter are described in detail.

Firstly, the main principles of calorimetric measurement methods are briefly reviewed in **Section II**. In **Section III**, the implementation of the double-jacketed calorimeter and the different control loops for the temperature difference across the test chamber walls, for the inlet temperature of the water and for the flow rate of the fluid are described in

detail. Finally, measurement results for a 99.2% efficient, 3kW AC-DC PFC rectifier with the realized calorimeter are presented in **Section IV**.

## II. CALORIMETRIC PRINCIPLES

Since power losses of electrical systems are dissipated as heat, they can be directly determined by measuring the generated heat. In calorimetric methods, there is a controlled medium (usually air or water) used to take over the heat produced by the tested device. Ideally, the heat is completely absorbed by this medium. The power dissipation ( $P_{loss}$ ) of the tested device can thus be determined as function of the temperature rise  $\Delta T$  between inlet and outlet water temperature, the mass density  $\rho$  and the flow rate  $\dot{V}$  of the coolant with

$$P_{loss} = c_p \cdot \dot{V} \cdot \rho \cdot \Delta T, \quad (1)$$

where  $c_p$  is the specific heat capacity of the fluid.

There are several sorts of calorimeters (e.g. [3], [5], [6]) which can be divided into three basic types (cf. Fig. 2). On the one hand, there is the open type calorimeter in which the device under test is placed directly in the measurement circuit and whereas the coolant has to be air. The main disadvantages with air as coolant are difficulties of measuring the heat capacitance, temperature rise and the volume flow, additionally air is very sensitive to environmental changes concerning humidity, temperature and density, which all in all leads to increasing measurement errors. The benefits are a simple construction and a fast response time. To improve the accuracy of the open type calorimeter, a balancing test is proposed in [13] and [8]. This balancing test is basically a reference measurement with a determined amount of power which is supplied to heaters in the test chamber. With these heaters the main measurement is reproduced. Therefore, the measured losses can be recalculated by the ratio of the steady state temperatures in both tests and the known power in the reference measurement. This type of calorimeter is often used for measuring induction machines with power losses up to several kilowatts ([13] and [14]).

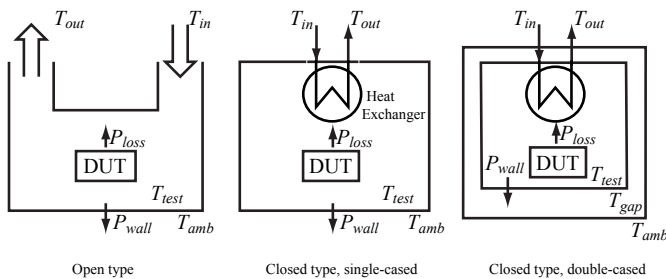


Figure 2. Schematic open, single-cased closed and double cased closed type.

On the other hand, there are two closed type calorimeters (cf. Fig. 2) which use a separate cooling loop (usually with water as coolant) for the heat exchange with the ambient, which leads to higher implementation complexity. Due to the higher heat capacitance of water compared to air, the settling

time is generally longer. The closed type is usually more accurate than the open type, as described e.g. in [1] and [?].

The double-cased closed type calorimeter allows an active control of the air temperature in the gap ( $T_{gap}$ ) between the cases and therefore to control the heat leakage across the walls, which leads to an improved accuracy of the calorimeter.

A major error source of all calorimeter types is heat leakage through the walls of the calorimeter ([?] and [4]). The heat flow  $P_{wall}$  through the walls can be estimated by

$$P_{wall} = \frac{T_{test} - T_{amb}}{R_{th,wall}}, \quad (2)$$

for the open type and the closed type single cased and by

$$P_{wall} = \frac{T_{test} - T_{gap}}{R_{th,wall}}, \quad (3)$$

for the closed type double-cased where  $T_{test}$  is the temperature in the test chamber,  $T_{amb}$  is the ambient temperature,  $T_{gap}$  is the air temperature in the air gap (cf. Fig. 2) and  $R_{th,wall}$  is the thermal resistance of the calorimeter walls (7).

There are some simplified scaling rules for a calorimeter for geometrical dimensioning of the calorimeter concerning the discussed power leakage through the insulation walls. The sensor accuracy can usually not be influenced since commercial sensors have a given uncertainty, the accuracy of the calorimeter can be optimized by a proper specification of the required test chamber volume of the calorimeter. There are basically two aspects under consideration, on one hand the thermal resistance of the test chamber walls, and on the other hand the time constant of the calorimetric measurement, which characterizes the settling time of the measurement. We assume a nominal test chamber volume  $V_{nom}$  with an inner test chamber surface  $A_{nom}$  and a given isolation wall thickness  $d_{nom}$ . By scaling the volume of the calorimeter equal in all directions by a factor  $k_{scal}$ , the inner surface of the calorimeter test chamber is scaled by  $k_{scal}^{2/3}$ .

The influence on the thermal resistance  $R_{th}$ , the thermal capacity  $C_{th}$  and the time constant  $\tau$  are summarized in table I.

Table I  
SCALING FACTORS

	$V_{nom}$	$A_{nom}$	$d_{nom}$	$R_{th}$	$C_{th}$	$\tau$
$d_{nom} = konst$	$k_{scal}$	$k_{scal}^{2/3}$	1	$k_{scal}^{-2/3}$	$k_{scal}^{2/3}$	1
$R_{th} = konst$	$k_{scal}$	$k_{scal}^{2/3}$	$k_{scal}^{2/3}$	1	$k_{scal}^{4/3}$	$k_{scal}^{4/3}$

It is obvious that a small test chamber volume leads to a shorter response time and also requires less isolation. As the thermal capacitance depends on the mass, the influence of the air in the test chamber compared to the influence of the walls is negligible. The dependence on the thermal capacity of the device under test is not considered in this scaling factor.

In addition, it is more difficult to provide a homogeneous chamber temperature as higher the volume of the test chamber is.

### III. IMPLEMENTATION

As already mentioned, this calorimeter is designed to measure power losses of a converter with an planned efficiency of higher than 99.0% and an output power between 1 kW and 10 kW. The lower measurement limit is at 10 W. The accuracy of the calorimeter should be better than  $\pm 0.4 \text{ W}$  ( $\pm 0.05\%$  with respect to full power of the device under test) for the verification of the system efficiency. In Fig. 3 an overview of the main design steps is given, which are described in more detail below.

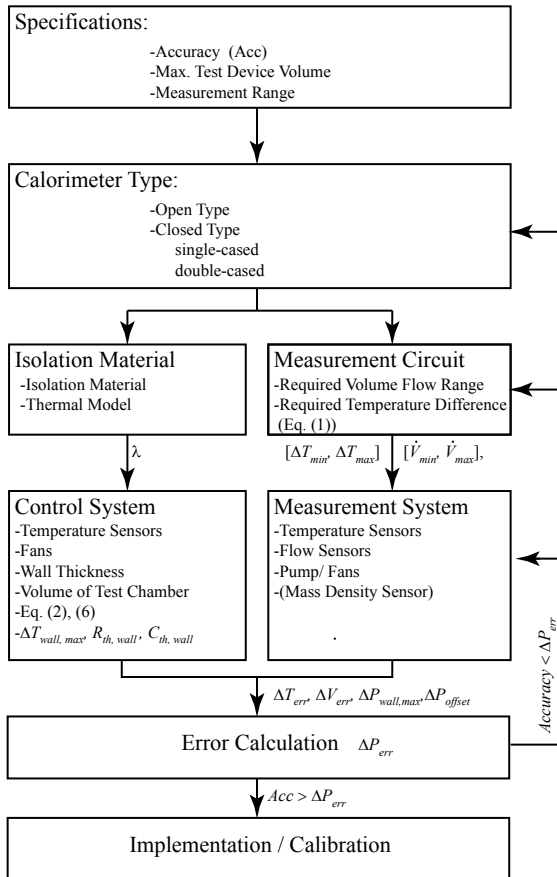


Figure 3. Main steps for the implementation of a calorimeter.

First, the maximum size of the test devices, the required measurement range and certainly the targeted accuracy are specified.

In a second step, the type of calorimeter that should be implemented is chosen in dependence of the specifications and the desired accuracy.

The isolation walls of the test chamber and the measurement circuit can be designed separately due to their individual functionality.

For the isolation walls, first the required thermal resistance can be calculated in dependence of the calorimeter type, the volume of the test chamber and the wall thickness. In the next step the sensors are evaluated with respect to their accuracy and to the required measurement range. Finally the heat leakage across the isolation walls can be determined taking the sensor accuracy and the inhomogeneous temperature

distribution in the test chamber, respectively in the air gap between the test chamber and the outer case into account. Furthermore, these two values also limit the heat leakage control for the double cased calorimeter.

For the measurement circuit first the volume flow range and the temperature range for the calorimeter are determined. Accordingly the sensors for the water inlet and outlet temperature and the volume flow sensor can be evaluated with respect to the required measurement range and accuracy.

Based on the estimated measurement uncertainty of the chosen sensors and the worst case power leakage over the test chamber walls, the measurement error of the calorimeter can be determined. If the measurement error is higher than the required accuracy, better isolation material or sensors with a higher accuracy have to be found, or the type of calorimetric measurement set-up has to be changed.

In a last step, the calorimetric system is implemented and calibrated with a known load like a resistive DC-load and accurate electric measurement equipment.

In our case, to reach the required accuracy, a double-jacketed closed type calorimeter is used. The presented design mainly contains two thermal insulating concentric boxes and a water circuit. The power losses of the device are transferred to the fluid via a heat exchanger (cf. Fig. 7) in the test chamber. Power losses can thus be determined by measuring the volume flow  $\dot{V}$  and temperature increase  $\Delta T$  of the fluid while it circulates through the test chamber with (1).

#### A. Materials and Dimensions

The fluid in the heat exchanger is water with the specific heat capacity of  $4.182 \cdot 10^3 \text{ J/kg K}$  and the mass density of  $\rho = 998.2 \text{ kg/m}^3$  at  $20^\circ\text{C}$ .

The dimensions of the box in which the device under test (DUT) is placed, are  $300 \text{ mm} \times 240 \text{ mm} \times 240 \text{ mm}$  (cf. Fig. 5). The material of the test chamber is expanded polystyrene with inner dimensions of  $385 \text{ mm} \times 390 \text{ mm} \times 500 \text{ mm}$  and a wall thickness of 50 mm. The specific thermal conductivity is  $0.035 \text{ W/Km}$  (cf. Tab.II). The outer box is made from extruded polystyrene plates (Ursa Foam, [19]) with inner dimensions of  $820 \text{ mm} \times 685 \text{ mm} \times 700 \text{ mm}$ , wall thickness of 40 mm and thermal conductivity of  $0.035 \text{ W/Km}$  (cf. Tab.II).

The used materials for realizing the measurement system are listed in Tab.II.

#### B. Power Measurement

As mentioned above, the power can be determined by measuring the flow rate of the fluid and the temperature increase of the fluid caused by the heating due to the losses of the test device.

Two temperature sensors (VIBROtemp, JUMO [15]) are placed in the tubes at the inlet and the outlet of the heat exchanger (cf. Fig. 7) to measure the water inlet and outlet temperature of the heat exchanger. These sensors are coupled with transducers which map the temperature between  $0^\circ\text{C}$  and  $100^\circ\text{C}$  on 0 V up to 10 V (dTransT03 BU, JUMO [15]). The accuracy of this system is better than  $\pm 0.1^\circ\text{C}$  for each sensor. In addition, the water circuit to the inner test chamber is isolated in order to prevent heat up of the coolant in the air

Table II  
USED MATERIALS FOR THE IMPLEMENTATION OF THE CALORIMETER.

	Type	Producer	Parameters
<b>Sensors</b>			
Water Temperature	VIBROtemp	JUMO [15]	Accuracy $\leq 0.1^\circ\text{C}$ Linearized: $0 \dots 100^\circ\text{C} \rightarrow 0 \dots 10\text{ V}$
Air Temperature	TMP275	Texas Instruments [16]	Accuracy $\leq 0.2^\circ\text{C}$ Measurement Range: $-40^\circ\text{C} \dots 125^\circ\text{C}$
Volume Flow	FCH-mPVDF	BIO-TECH[17]	Accuracy $\leq 2\%$ MR: $0.01\text{ l/min} \dots 0.9\text{ l/min}$ Repeatability $\leq 0.5\%$
<b>Insulation Materials</b>			
Inner Chamber	Insulation Box	STOROpac[18]	Inner dimensions: $385\text{ mm} \times 390\text{ mm} \times 500\text{ mm}$ Wall Thickness: $50\text{ mm}$ Thermal conductivity $\lambda$ : $0.035\text{ W/Km}$
Outer Chamber	Ursa Foam	Coop[19]	Dimensions: $1250\text{ mm} \times 600\text{ mm} \times 40\text{ mm}$ Thermal conductivity $\lambda$ : $0.035\text{ W/Km}$
<b>Water Circuit</b>			
Pump	BPS-1	Levitronix [20]	Rotary speed regulated Max. pressure: $3.8\text{ bar}$
Heat Exchanger	airplex pro 240	Aqua-computer[21]	Dimensions: $120\text{ mm} \times 276\text{ mm} \times 30\text{ mm}$

gap. A flow meter is used (FCH-m-PVDF, BIO-TECH [17]) to measure the flow rate with a measurement range of  $0.01\text{ l/min}$  up to  $0.9\text{ l/min}$  and accuracy better than  $\pm 2\%$ .

The vertex accuracy of the power measurement can thus be calculated with:

$$\frac{P_{err}}{P_{meas,eff}} = \frac{\Delta T_{err}}{\Delta T_{eff}} + \frac{\Delta T_{err} \cdot \dot{V}_{err}}{\Delta T_{eff} \cdot \dot{V}_{eff}} + \frac{\dot{V}_{err}}{\dot{V}_{eff}} \quad (4)$$

whereas  $P_{err}$  is the error in the power measurement,  $\Delta T_{err}$  is the measurement error for the temperature difference between inlet and outlet temperature of the test chamber and  $\dot{V}_{eff}$  is the accuracy of the volume flow sensor. Furthermore,  $P_{meas,eff}$  is the effective measured power,  $\Delta T_{eff}$  is the effective measured temperature difference and  $\dot{V}_{eff}$  is the effective volume flow. This leads to an accuracy without calibration of  $3.02\%$  if  $\Delta T_{eff}$  is assumed to be  $20^\circ\text{C}$ .

With respect to the Gaussian law of error propagation the error in the measurement can be calculated with

$$\Delta y(x_1, x_2, \dots) = \sqrt{\left(\frac{\delta y}{\delta x_1} \cdot \Delta x_1\right)^2 + \left(\frac{\delta y}{\delta x_2} \cdot \Delta x_2\right)^2 + \dots} \quad (5)$$

Accordingly, the estimated measurement errors are

$$\frac{\Delta P_{err}}{P_{meas,eff}} = \sqrt{\left(\frac{\Delta T_{err}}{\Delta T_{eff}}\right)^2 + \left(\frac{\dot{V}_{err}}{\dot{V}_{eff}}\right)^2} = 2.236\% \quad (6)$$

This value is the most probable (approximately  $3\sigma$ ), and therefore used for dimensioning the calorimeter.

### C. Leakage Heat Flow through the Walls

As already mentioned, one source of error in the calorimetric measurement is the heat leakage through the test chamber walls. The test chamber needs a proper isolation to minimize this effect. The thermal resistance of the test chamber walls can be calculated with (7) and the heat flow across the test chamber walls can be minimized, the thicker the test chamber walls are. However, the test chamber walls have a thermal capacity (8) which also increases, the thicker the test chamber walls are chosen.

$$R_{th} = \frac{d_{wall}}{\lambda_{wall} \cdot A_{wall}} \quad (7)$$

$$C_{th} = c_{th} \cdot V \cdot \rho \quad (8)$$

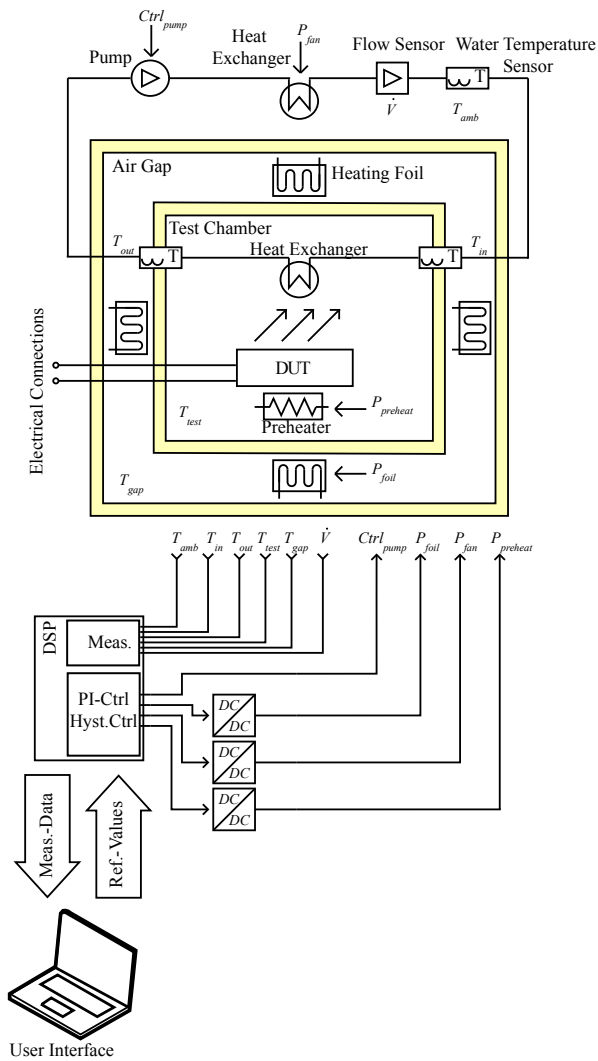
$$\tau = C_{th} \cdot R_{th} \quad (9)$$

Therefore, the time constant (9) for the system increases proportional with the square of the thickness of the walls. This means that it makes no sense to just increase the thickness of the walls.

In our case a double-cased calorimeter is implemented. This enable the temperature difference across the test chamber walls to be minimized with respect to the sensor accuracy and thermal distribution in the chamber as in the air gap between inner and outer case. The thickness can be estimated when seeking a short settling time and in order to minimize the leakage heat flow through the walls.



a) Implementation of the Calorimetric Measurement System



b) Integration of Water Cooled Test Devices

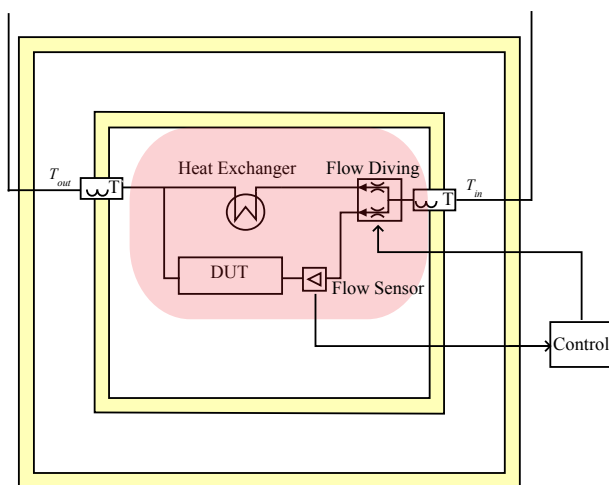


Figure 4. a) Schematic implementation of the double jacketed calorimeter with a water cooled circuit for power measurement, and principle control and measurement circuit. b) Integration of an additional flow sensor and a flow diverging for the calorimetric measurement of water cooled systems.

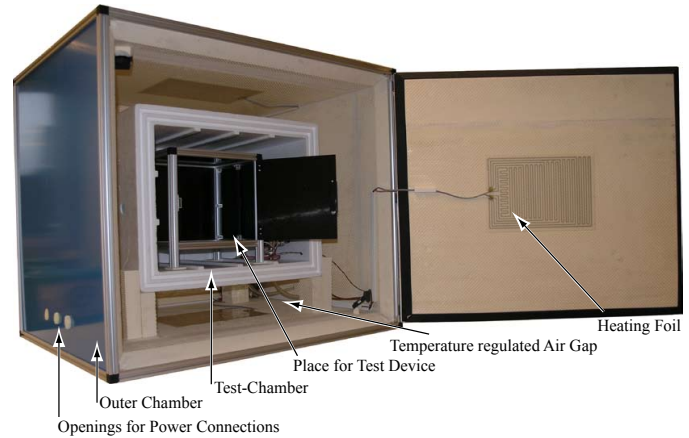


Figure 5. Realized double-jacketed calorimeter for accurate power-loss measurement of high efficient converter systems with an output power of several kW.

As discussed above the leakage heat flow through the walls is dependent on the temperature distribution in the test chamber as well as in the air gap between the test chamber and the outer case. An air channel is introduced to channel the air flow in the test chamber and reach a homogeneous wall temperature. The test device is placed in this channel as presented in Fig. 6 and Fig. 7. The test device basically heats up the air which is forced through the heat exchanger. After the heat exchanger there is almost no more heating influence on the air temperature and therefore, the air temperature along the inner surface of the test chamber stays constant.

Heating foils are used with a total power of 90 W to heat up the gap between the test chamber and the outer case. Eight digital temperature sensors (TMP275, Texas Instruments [16]) are used to measure the inner and outer wall temperature. These sensors have an accuracy better than  $\pm 0.15^\circ\text{C}$  and a resolution of  $0.0625^\circ\text{C}$ . The temperature difference between

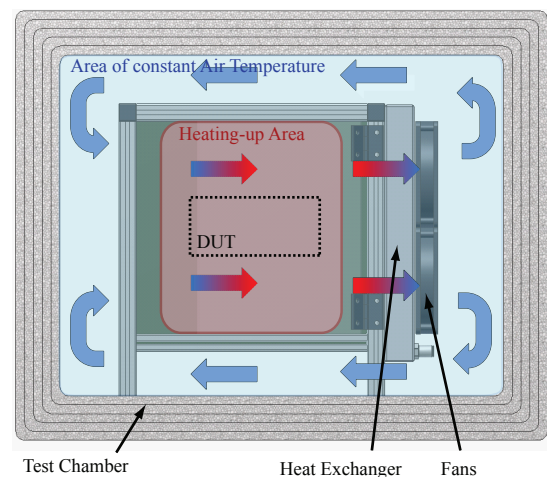


Figure 6. Principle of the air circulation in the test chamber.

inside and outside of the test chamber is limited to  $0.3^\circ\text{C}$  with a hysteresis control loop. The thermal resistance is estimated to  $1.33\text{ K/W}$  with (7).

Measurements show that the thermal resistance is reduced by the inlets and outlets for the water, the temperature sensing as well as the electrical connections to approx.  $0.82 \text{ K/W}$ . The resulting calculated power fluctuation via the wall is approximately  $0.365 \text{ W}$  for a temperature difference of  $0.3^\circ\text{C}$ . However, due to the temperature difference across the heat exchanger, the temperature variation is within  $0.5^\circ\text{C}$  in the test chamber. Therefore, the average temperature is used for the temperature control. The gap heating with the foils leads to a almost constant temperature which differs only within  $0.15^\circ\text{C}$ .

A better homogenization of the air temperature in the test chamber allows a better temperature wall control and therefore increases the accuracy of the calorimeter and is under investigation.

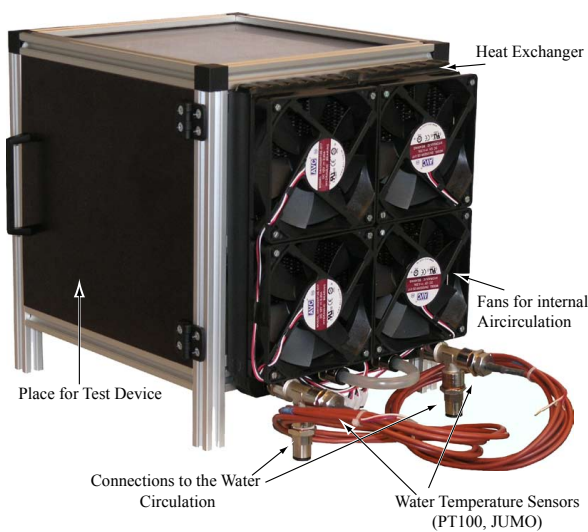


Figure 7. Air channel, in which the test converter system is placed. The air circulates through this chamber to guarantee a homogeneous wall temperature on the surface of the inner chamber.

#### D. Data Acquisition

A Java GUI (on a PC) for data acquisition connected to a control board with a DSP has been implemented (cf. Fig. 8). The data is recorded and sensed with the DSP connected to the sensors. The Java GUI reads the data from the DSP and stores it in a text file. The reference values for the input water temperature and for the flow rate are set with this program.

The recorded measurements are

- the air temperature in the space between the inner and the outer chamber
- the air temperature in the test chamber,
- the flow rate
- the water inlet and outlet temperature

This GUI also provides the possibility of a real-time observation of the recorded data and calculates the dissipated power in the test chamber.

#### E. Thermal and Flow Control

In order to increase the accuracy and to reduce the settling time (which characterizes the time until the system reaches the

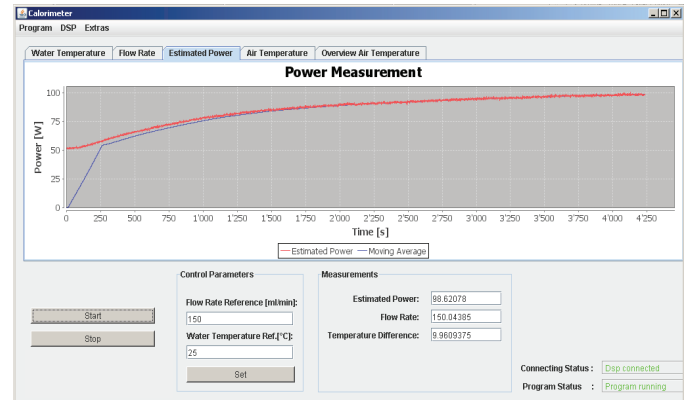


Figure 8. Implemented Java GUI for data acquisition.

thermal equilibrium) of the calorimeter, a stabilizing control for the volume flow and for the inlet water temperature are set up. In addition, a preheating system for the thermal chamber is presented.

To control the volume flow, a highly accurate flow sensor in combination with a duty cycle controlled pump is used. The implemented PI control loop controls the volume flow on an almost constant average value. The reference value for the rotary speed of the pump is controlled with the PI-control.

The parameters for the PI-control were selected having considered the step-response with Ziegler-Nichols method and further fine tuning.

The calorimetric measurement is very sensitive to temperature changes and therefore it is important to stabilize the inlet water temperature on a constant value during the whole test time to reach thermal equilibrium and the highest accuracy as soon as possible. In a first step the fans on the outer heat exchanger are controlled resulting in controlled cooling of the warm water coming from the calorimeter. The desired inlet water temperature should be around  $1^\circ\text{C}$  above ambient temperature. Due to the fact that the inlet water temperature still fluctuates by about  $0.2^\circ\text{C}$  investigations into the inlet water temperature control are continuing.

The preheating system of the test chamber mainly contains an aluminum heatsink on which three resistors are placed. The expected losses of a device under test have to be known to use the preheating system. In a first step the calorimetric test chamber is can be preheated to a certain temperature. When about 90% of the expected losses are reached, the power dissipated by the preheating resistors is set to zero. The test device does not therefore have to heat up the whole test chamber by itself and accordingly the settling time is reduced, especially for measurements at the lower limit of the measurement range.

The necessary PI- and hysteresis controllers are implemented on the DSP whereas the reference values can be set via the presented Java-GUI.

#### F. Implementation with water cooled test device

First considerations on the adaptations made to use that type of calorimeter for measuring power losses of water cooled test devices are given. The main principle is presented in Fig. 4

b). The test device is still placed in the test chamber and the water cooler of the test system is connected in parallel to the heat exchanger. The pressure drop across the test device and the heat exchanger as well as the pump characteristics have to be known to guarantee secure operation concerning the test chamber and device temperature. Furthermore, an additional flow sensor and a controllable flow diving are necessary to control the cooling respectively the water flow.

#### IV. CALIBRATION AND MEASUREMENTS

The four fans placed in the test chamber to produce the airflow as presented in Fig. 7, consume 5.02 W. Each of the four temperature sensors has a power dissipation of 40 mW. As mentioned above, the thermal resistance of the wall is around 0.82 K/W. The power fluctuation over the walls can be minimized to 0.365 W with  $T_{wall} = 0.3^\circ\text{C}$ . This leads to a measurement offset of about  $5.02\text{ W} - 0.365\text{ W} = 4.655\text{ W}$ . The offset caused by the internal ventilation and the sensors can be minimized by calibration. The offset caused by the temperature difference across the walls has to be accounted as measurement uncertainty. As already showed in the previous section the uncertainty caused by sensing is 2.236 %. The flow rate sensor has an accuracy of better than 0.5 % for repetitive measurements under same conditions. As a consequence, the measurement uncertainty recalculates with (6) to 1.118 %. The overall measurement error calculates to

$$\frac{P_{err,tot}}{P_{meas}} = \frac{P_{wall}}{P_{meas}} + \frac{\Delta P_{sens,err}}{P_{meas}} \quad (10)$$

The absolute measurement error due to the heat leakage across the test chamber walls is equal over the whole measurement range and causes a high relative measurement fault for the lower power measurements. The relative uncertainty of the sensors is about the same for all power measurements which leads to a constant percentage measurement error over the complete measurement range.

The accuracies given in Fig. 9 can be achieved theoretically for different power losses. It also can be seen that power losses as low as 9.4 W can be measured with the required accuracy of 5% compared to the measured power losses.

Table III  
MEASUREMENTS WITH OHMIC DC-LOAD.

Measurements DC-Input (110 $\Omega$ -Resistance)				
DC Input	11.190 W	39.538 W	52.373 W	98.094 W
Measured	11.110 W	39.750 W	52.120 W	97.720 W
$\Delta P$	0.079 W	0.288 W	0.252 W	0.374 W
Error [%]	0.706%	0.728%	0.481%	0.381%

To calibrate the calorimeter, a 110  $\Omega$  resistor is used as a test device. The voltage and the current across this resistance are measured with highly accurate, calibrated voltage meters (Keithley, accuracy  $\pm 0.01\text{ mV}$ , [22]) in combination with a calibrated shunt resistance (Burstner, fault tolerance  $\pm 0.02\%$ , [23]). Each measurement takes about 3 h-5 h measurement time.

The accuracy of the measurements with a resistive DC-load is within  $\pm 0.4\text{ W}$  (Tab. III).

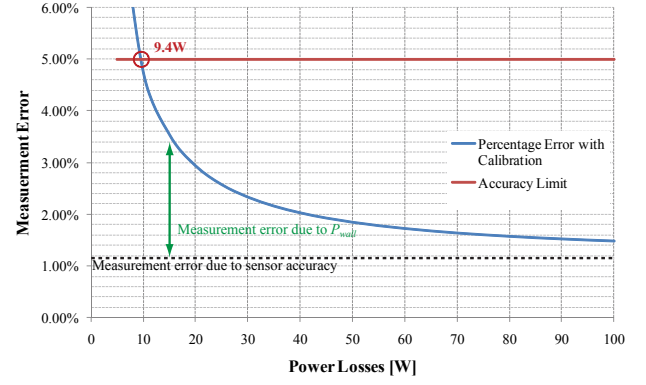


Figure 9. Theoretical worst case accuracy for different power losses. Measurement error due to the heat leakage across the test chamber walls (green.). Measurement error due to the accuracy of the sensors.

After calibration, reference measurements with a resistive DC-load have been performed for different powers. The results are presented in Fig. 9. The percentage measurement error is always below the calculated worst case accuracy. Furthermore the absolute measurement error for loads less than 50W is less than 0.4 W. The calorimetric measurement is within  $\pm 1\%$ , due to the uncertainty of the used sensors for higher loads. Therefore, the overall accuracy of the calorimeter is even higher than expected.

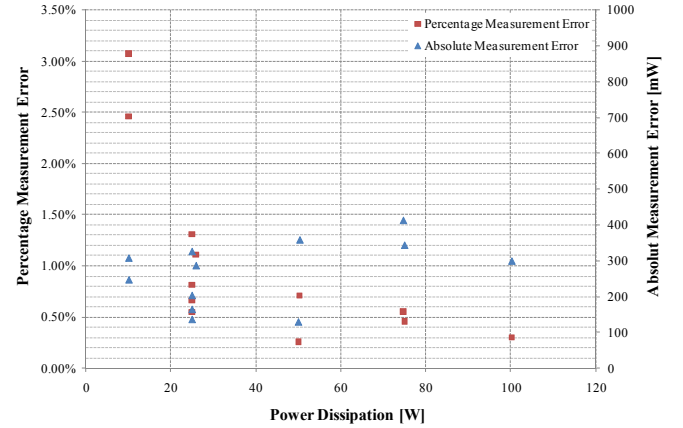


Figure 10. Calorimetric measurements for different loads. The percentage error (red) for a resistive DC-Load. The absolute measurement error (blue) for a resistive DC-Load.

Initial measurements with a single-phase PFC rectifier have been performed [24]. The power losses of the first prototype have been measured to about 15.0 W at an output power of 1.6 kW. The measurement curve is presented in Fig. 11 where after 4 h steady state has been reached. A reference measurement with a determined power loss was made to confirm and validate the measured results. Additional measurements of test devices with power losses up to about 190 W have been performed.



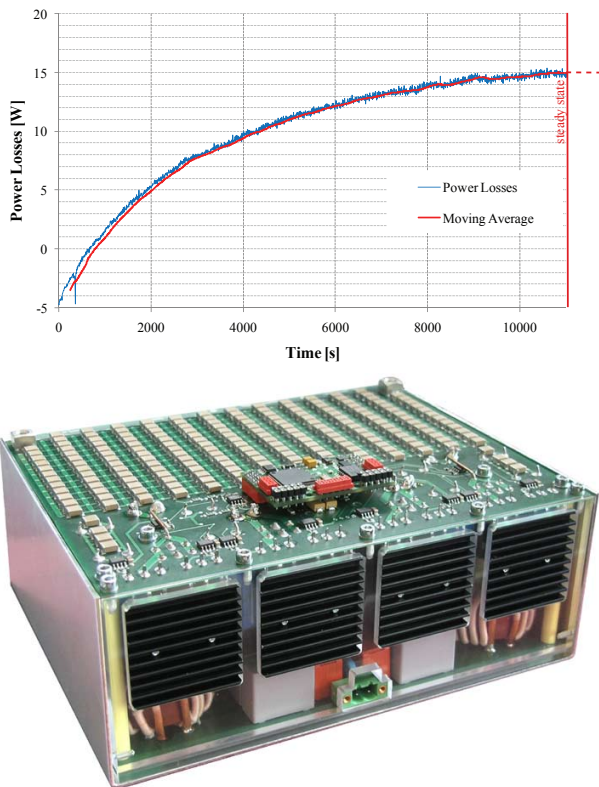


Figure 11. Resulting measurement curve for the single-phase PFC rectifier [24].

## V. CONCLUSION

In this paper, the design and realization of a highly accurate calorimetric power loss measurement system for power converter is presented. The calorimeter allows a power loss measurement for highly efficient power electronic systems with a full range power between 1 kW and 10 kW and power losses from 10 W up to 100 W within  $\pm 0.4$  W or 1% accuracy. The theoretical analysis of the measurement system is discussed in detail. The system is calibrated and the theoretical approach is validated by measurements. Furthermore the possible connection for water cooled systems is proposed.

The accuracy of the calorimeter can be improved by implementing a better air temperature homogenization in the inner test chamber and an improved water inlet temperature control.

## REFERENCES

- [1] C. Xiao, G. Chen, and W. Odendaal, "Overview of power loss measurement techniques in power electronics systems," in *IEEE Transactions on Industry Applications*, vol. 43, 2007, pp. 657–664.
- [2] P. Malliband, D. Carter, B. Gordon, and R. McMahon, "Design of a double-jacketed, closed type calorimeter for direct measurement of motor losses," in *7<sup>th</sup> International Conference on Power Electronics and Variable Speed Drives*, no. 456, 1998, pp. 212–217.
- [3] S. Weier, M. Shafi, and R. McMahon, "Precision calorimetry for the accurate measurement of losses in power electronic devices," in *Industry Applications Society Annual Meeting (IAS)*, 2008, pp. 1–7.
- [4] S. Weier, R. McMahon, and P. Malliband, "Calorimetry for power electronics," in *Proceedings of the 41<sup>st</sup> International Universities Power Engineering Conference (UPEC)*, 2006, pp. 608–612.
- [5] G. Chen, C. Xiao, and W. Odendaal, "An apparatus for loss measurement of integrated power electronics modules: design and analysis," in *Conference Records of the 37<sup>th</sup> Annual Industry Applications Conference (IAS)*, 2002, pp. 222–226.
- [6] P. Wolfs and Q. Li, "Precision calorimetry for power loss measurement of a very low power maximum power point tracker," in *Australasian Universities Power Engineering Conference (AUPEC)*, 2007, pp. 1–5.
- [7] P. McLeod, K. J. Bradley, A. Ferrah, R. Magill, J. G. Clare, P. Wheeler, and P. Sewell, "High precision calorimetry for the measurement of the efficiency of induction motors," in *Proceedings of the 33<sup>rd</sup> Industry Applications Conference (IAS)*, 1998, pp. 304–311.
- [8] A. Jalilian, V. J. Gosbell, B. S. P. Perera, and P. Cooper, "Double chamber calorimeter (DCC): a new approach to measure induction motor harmonic losses," in *IEEE Transactions on Energy Conversion*, vol. 14, no. 3, 1999, pp. 680–685.
- [9] A. V. den Bossche, "Flow calorimeter for power electronic converters," in *Proceedings of the EPE Conference*, 2001, pp. 27–29.
- [10] W. Cao, K. J. Bradley, and A. Ferrah, "Development of a high-precision calorimeter for measuring power loss in electrical machines," in *IEEE Transactions on Instrumentation and Measurement*, vol. 58, no. 3, 2009, pp. 570–577.
- [11] U. Badstuebner, J. Biela, and J. Kolar, "An Optimized, 99 % Efficient, 5 kW, Phase-Shift PWM DC-DC Converter for Data Centers and Telecom Applications," in *International Power Electronics Conference (IPEC - Sapporo)*, jun 2010.
- [12] P. D. Malliband, N. P. van der Duijn Schouten, and R. A. McMahon, "Precision calorimetry for the accurate measurement of inverter losses," in *The 5<sup>th</sup> International Conference on Power Electronics and Drive Systems*, 2003, pp. 321–326.
- [13] D. R. Turner, K. J. Binns, B. N. Shamsadeen, and D. F. Warne, "Accurate measurement of induction motor losses using balance calorimeter," in *IEE Proceedings B [see also IEE Proceedings-Electric Power Applications] Electric Power Applications*, vol. 138, no. 5, 1991, pp. 233–242.
- [14] K. Bradley, A. Ferrah, R. Magill, J. Clare, P. Wheeler, and P. Sewell, "Improvements to precision measurement of stray load loss by calorimeter," in *9<sup>th</sup> International Conference on Electrical Machines and Drives, 1999. (Conf. Publ. No. 468)*, 1999, pp. 189–193.
- [15] JUMO Instrument Co. Ltd. [Online]. Available: <http://www.jumo.ch/>
- [16] Texas Instruments. [Online]. Available: <http://www.ti.com/>
- [17] BIO-TECH. [Online]. Available: <http://www.btflowmeter.com/>
- [18] STOROPack. [Online]. Available: <http://www.storopack.ch/>
- [19] [Online]. Available: <http://www.coop.ch/pb/site/bauhobby>
- [20] Levitronix. [Online]. Available: <http://www.levitronix.com/>
- [21] Aqua-Computer. [Online]. Available: <http://aquacomputer.de/>
- [22] Keithley Instruments Inc. [Online]. Available: <http://www.keithley.ch/>
- [23] Burster Präzisionsmesstechnik gmbh & co. [Online]. Available: <http://www.burster.de/>
- [24] J. Biela, J. W. Kolar, and G. Deboy, "Optimal design of a compact 99.3% efficient single-phase PFC rectifier," in *IEEE Applied Power Electronics Conference (APEC)*, 2010.